8-1-1988

Simulation of the Polarizable-Ion Dynamics of Rb_2ZnCl_4

P. J. Edwardson
U.S. Naval Research Laboratory, Washington, D.C.

John R. Hardy
University of Nebraska - Lincoln

Simulation of the polarizable-ion dynamics of Rb_2ZnCl_4

P. J. Edwardson
Condensed Matter Physics Branch, U.S. Naval Research Laboratory, Washington, D.C. 20375-5000

J. R. Hardy
Department of Physics, University of Nebraska at Lincoln, Lincoln, Nebraska 68588-0111
(Received 23 December 1987; revised manuscript received 25 March 1988)

The promotion yet prevention of structural stability in the paraelectric phase of Rb_2ZnCl_4 by ionic polarizability is explored with both constant-lattice and variable-lattice simulations. As many as 168 ions ($3\times1\times2$ cells) under periodic boundary constraints are allowed to polarize in nonlinear response to forces which are obtained from the electron-gas model of Gordon and Kim. No assumption about the rigidity of the $ZnCl_4^{2-}$ ion is made. The cause of polarization catastrophe in linear models is examined, and a cure is implemented via nonlinearity of the dipole moment versus field strength. Among the observations are a soliton and cell-multiplying instabilities against rotations and translations of the $ZnCl_4^{2-}$ ions.

I. INTRODUCTION

A rigid-ion simulation of the paraelectric high-temperature phase of Rb_2ZnCl_4 was recently reported in which several characteristics of the possible disordered solid were poorly or not at all reproduced.[1] The short-range potentials determined from the electron-gas model of Gordon and Kim produced a Zn^{2+}—Cl^- bond that was too long, and relaxation, within symmetry constraints, of the forces on the ions led to very distorted $ZnCl_4^{2-}$ ions. These two shortcomings were corrected by scaling the short-range part of the Zn^{2+}—Cl^- pair potential, but then a relaxation within constraints caused large rotations of the tetrahedral ions away from their experimentally determined average orientations. The final failure of the model occurred when this relaxed structure was used as the starting point for a dynamics simulation. One quarter of the chloride ions moved from their initial sublattice to a completely different one, destroying the integrity of the $ZnCl_4^{2-}$ ions. Thus, there were two forces missing from the rigid-ion model: those that keep the $ZnCl_4^{2-}$ ions intact; and those that keep the same ions in their experimentally determined orientations.

One possible explanation for the failure of that simulation to produce something like the experimental structure is that charge is transferred within the $ZnCl_4^{2-}$ ion to reduce the effective charge of the zinc ion and increase that of the chloride ion. Indeed, evidence for this charge transfer can be found in determinations of the *monopoles* that should be placed at the experimentally determined positions of the ions in Cs_2ZnCl_4 (Ref. 2) and in Rb_2ZnCl_4 (Ref. 3) in order to best reproduce the electromagnetic field gradients as measured by nuclear magnetic resonance. Both of these studies suggest that the charge on the zinc ion is $1+$ and on the chloride ion is $\frac{3}{4}-$.

A more plausible explanation of the failure of the rigid-ion simulation was found to be its neglect of the polarizability of the ions. Polarizable ions would favor shorter Zn^{2+}—Cl^- bonds because the chloride ions would seek stronger fields nearer the zinc ion. Energy of polarization would have to be overcome to disassociate the ion, and bond-angle bending would be stiffer from repulsion between Cl^- dipole moments. Furthermore, comparison of the fields at the sites of the chloride ions in the experimentally determined average structure to the fields in the simulation strongly suggested that polarizable ions would favor the experimental structure, i.e., the displacements of one quarter of the chloride ions mentioned above were from sites with strong fields to sites with zero fields. Thus, ionic polarizability is likely the source of both forces that were missing in the rigid-ion simulation.

Results presented here support the hypotheses that the $ZnCl_4^{2-}$ ion may be considered a conglomerate of polarizable ions, and that polarizability plays a key role in the orientation of the $ZnCl_4^{2-}$ ions in the solid and in the transformations of the paraelectric phase upon cooling. Constant-lattice and variable-lattice simulations of the dynamics of up to 168 polarizable ions with periodic boundary constraints are reported. Short-range forces are obtained from the electron-gas model of Gordon and Kim and no assumption about the rigidity of the $ZnCl_4^{2-}$ ions is made. The cause of polarization catastrophe in the linear-polarizability approximation is discussed and an appropriate nonlinear model is used. Simulations with normal and reduced polarizabilities are compared and the roles of induced dipole moments in structural details are examined. A zone-center instability and a probable cell-multiplying instability are found and their relevance to disorder in the paraelectric phase and the transformations of this solid upon cooling is discussed.

II. METHOD

The mass of an ion is assumed to be at the nucleus, and the effect of an induced dipole moment is to change the center of force between a "shell" of an ion's electrons and the other force centers in the crystal. Pair potentials are determined from the electron-gas model of Gordon and Kim,[4] and are then fitted to an analytic function which is

described in Ref. 1. For the present study, all electrons of an ion are included in its shell because the electron-gas potentials separate naturally into electron-electron, electron-nuclear, and nuclear-nuclear parts. Approximate separation of potentials into shell-shell, shell-core, and core-core parts should be possible to do accurately *ab initio* once criteria for determining shell charges are defined, but that is not attempted here.

The electron-gas model requires electron densities of the individual ions. The Hartree-Fock densities of isolated zinc and rubidium ions were used,[5] but a chloride-ion density contracted by a Watson-shell potential gives a better description of the ion in a solid than does the isolated-ion density.[6] A Watson potential is that of a shell of charge $1+$ to simulate a spherically averaged effect of the crystal environment on the potential energy of the electrons in the ion. The electrostatic potential near the chloride-ion sites in Rb_2ZnCl_4 resembles a Watson-shell plateau with an additional tilt away from the zinc ion. The tilt, i.e., the presence of a field, is included as a dynamical variable in the present simulations.

The charge of the shell is set at $1+$ because that is the charge that surrounds the chloride ion in the neutral solid—different reasoning than used by Watson.[7] The radius of the shell is determined by requiring the constant electrostatic potential inside to equal the potential at the ion site in the crystal. The contributions by monopoles to the potentials at the three kinds of chloride-ion sites in the experimentally determined average structure of paraelectric Rb_2ZnCl_4 are 0.328 (two equivalent sites), 0.331, and 0.349 a.u. For comparison, the electrostatic potential at the chloride-ion site in NaCl is 0.328 a.u.

An additional contribution to the potential experienced by the electrons of the chloride ion is that of the dipole moments of the other ions in the crystal. We estimated this potential to be about 0.02 a.u. by halving the per-ion electrostatic energy of interaction between all monopoles and all dipoles. The dipoles were induced by both electrostatic and short-range forces using the model described below. Half of that energy was used in the assumption that the energy per ion is partitioned equally between interaction of the ion's dipole and monopole with other monopoles and dipoles, respectively. Thus, the chloride-ion density was determined with the program of Liberman *et al.*[8] using a Watson shell with an inner potential of 0.35 a.u.

Let q_i be the charge of the shell (all of the electrons) of ion i. The displacements $\Delta\mathbf{r}$ of the shells from their associated cores (nuclei) can be assumed to be small, so the potential energy of the crystal can be expanded as a Taylor series in those displacements. In terms of the dipole moments on the ions $\boldsymbol{\mu}_i = q_i \Delta\mathbf{r}_i$, the expansion through second order is

$$
\begin{aligned}
U = & \sum_i \varepsilon_i(\mu_i) \\
& + \tfrac{1}{2} \sum_{i,j} \{ u_{ij} + 2(\boldsymbol{\mu}_i \cdot \nabla_i / q_i)(u_{ij}^{-+} + u_{ij}^{--}) \\
& \quad + [(\boldsymbol{\mu}_i \cdot \nabla_i / q_i)^2 (u_{ij}^{-+} + u_{ij}^{--}) \\
& \quad + (\boldsymbol{\mu}_i \cdot \nabla_i / q_i)(\boldsymbol{\mu}_j \cdot \nabla_j / q_j) u_{ij}^{--}] \} , \qquad (1)
\end{aligned}
$$

where ε_i is the change in self-energy of the ion caused by the induction of a dipole moment, u_{ij}^{-+} and u_{ij}^{--} are the interaction energies of shell i with core j and shell j, respectively, and u_{ij} is the summation of core-core, shell-shell, and both core-shell energies, i.e., u_{ij} is the energy of interaction that rigid ions would have. These potential energies are functions of the intercore separations $r_{ij} = |\mathbf{r}_i - \mathbf{r}_j|$, and the subscripts on the gradient operators in Eq. (1) indicate which ion's core coordinates are the variable of differentiation. Other than self-energy and rigid-ion interactions, Eq. (1) includes interactions of dipoles with monopoles, gradients of the monopole "fields," and other dipoles. We will use the word field loosely to include nonelectrostatic contributions also.

It is expected that including all of the electrons in the shells might cause significant errors only in the intraionic forces, i.e., those within the $ZnCl_4^{2-}$ ions. Dependence in Eq. (1) on the shell charges can only be found in the short-range interactions and in the long-range part of the field-gradient interaction. The shell charges cancel in the long-range monopole-dipole and dipole-dipole interactions, which are essentially equivalent to a point-dipole model. Since interionic (as opposed to intraionic) separations are large in Rb_2ZnCl_4, it is likely that only long-range monopole-monopole and monopole-dipole interactions are important, and those are well described in the present approximation, independent of the choice of shell charges.

The equations of motion of the core positions, $m_i \mathbf{a}_i = -\nabla_i U$, for a constant-lattice simulation and their generalization for a constant-stress simulation,[9] are obtained easily from Eq. (1) and do not need to be discussed further. With the assumption that the shells are massless, the equations of motion for the dipole moments are $\partial U / \partial \mu_{i\mu} = 0$, or

$$
\begin{aligned}
\frac{\partial \varepsilon_i}{\partial \boldsymbol{\mu}_i} = & -(\nabla_i / q_i) \sum_j \{ u_{ij}^{-+} + u_{ij}^{--} \\
& + [(\boldsymbol{\mu}_i \cdot \nabla_i / q_i)(u_{ij}^{--} + u_{ij}^{-+}) \\
& + (\boldsymbol{\mu}_j \cdot \nabla_j / q_j) u_{ij}^{--}] \} , \qquad (2)
\end{aligned}
$$

where $(\partial / \partial \boldsymbol{\mu})_\nu = \partial / \partial \mu_\nu$.

The interactions with field gradients are included but induction of higher multipole moments by field gradients is not allowed. Thus, the self-energy change ε_i is a function of the induced dipole moment μ_i only, and that function may be determined by placing an isolated ion in a uniform *electric* field, even though the "fields" in Eq. (2) have nonelectrostatic contributions. The self-energy and dipole moment of an ion are related parametrically through the uniform-field strength $\mathcal{E}$ by

$$
\frac{d\varepsilon}{d\mathcal{E}} = \mathcal{E} \frac{d\mu}{d\mathcal{E}} \qquad (3)
$$

and

$$
\frac{d\varepsilon}{d\mu} = \mathcal{E} . \qquad (4)
$$

If the function $\mu(\mathcal{E})$ were known, Eqs. (2) and (4) would determine the value of the equivalent-field strength

$\mathcal{E}$ at each ion site. The first few terms of the Taylor series might seem a logical choice. The Taylor series of the induced dipole moment and self-energy change of a spherical ion in a uniform field are[10]

$$\mu=(\alpha+\tfrac{1}{6}\gamma\mathcal{E}^2+\cdots)\mathcal{E} \text{ and } \varepsilon=\tfrac{1}{2}\alpha\mathcal{E}^2+\tfrac{1}{8}\gamma\mathcal{E}^4+\cdots . \tag{5}$$

The parameter α is the dipole polarizability of the ion and γ is the second dipole hyperpolarizability. The linear shell model, which assumes harmonic coupling of the core and shell, is equivalent to the approximation made by keeping the terms that involve the polarizability α only. This model has been used successfully in simulations of crystals with the rocksalt structure.[11,12]

The linear approximation reduces Eqs. (2) to a set of equations linear in the fields at the ion sites. However, in structures with low symmetry, that approximation invites a polarization catastrophe.[11,13] The source of this catastrophe can easily be seen by considering a point-dipole model of an ion: Each positive self-energy $\alpha\mathcal{E}^2/2$ is exactly canceled by dipole-dipole interactions $-\boldsymbol{\mu}\cdot\boldsymbol{\mathcal{E}}/2$, with $\boldsymbol{\mu}=\alpha\boldsymbol{\mathcal{E}}$, leaving only the dipole-monopole interactions $-\boldsymbol{\mu}\cdot\boldsymbol{\mathcal{E}}_0$, where $\boldsymbol{\mathcal{E}}_0$ is the field at the ion arising from other monopoles. Thus, the dipole moments will seek an arrangement in which dipole-dipole interactions induce infinite moments which align with monopole fields.

To remove the catastrophe from the present model, it appears that $\mu(\mathcal{E})$ must have negative curvature at high field strengths. This appears to work by attenuating growth of the dipole moment with field strength (thus dipole-monopole and dipole-dipole interactions) before attenuating the growth of the positive self-energy, because the negative curvature appears in a higher power of $\mathcal{E}$ in the Taylor series for the self-energy than it does in the series for the dipole moment. It is probable that negative curvature is only mimicking the effect of processes not described in a dipole-only model.

The negative curvature required in $\mu(\mathcal{E})$ is not obtained by including in Eqs. (5) the terms containing the second dipole hyperpolarizability γ, because those are certainly positive.[14] Lacking further information about the function $\mu(\mathcal{E})$, we have invented a tractable form that allows the polarizability and the second hyperpolarizability to be positive, has negative curvature at high field strengths, and satisfies (barely) the requirement that the function increase monotonically:

$$\mu(\mathcal{E})=\frac{\alpha}{a}\int_0^{a\mathcal{E}}(1+b\omega^2)e^{-\omega^2}d\omega$$
$$=\frac{\sqrt{\pi}\alpha}{2a}\left[1+\frac{b}{2}\right]\operatorname{erf}(a\mathcal{E})-\frac{\alpha b}{2}\mathcal{E}e^{-(a\mathcal{E})^2}, \tag{6}$$

where α is the polarizability of the ion, and a and b are parameters. An undesirable property of this function is that the dipole moment reaches a saturation value at large field strength. However, we emphasize that dipole moments stay far from saturation in practice. It is the slight negative curvature in $\mu(\mathcal{E})$ before saturation that prevents a catastrophe. The second hyperpolarizability from Eq. (6) is $\gamma=2\alpha a^2(b-1)$, and the saturation dipole moment is $\alpha(1+b/2)\sqrt{\pi}/(2a)$.

Values of the three parameters α, a, and b that determine $\mu(\mathcal{E})$ for each ion must be obtained. The polarizabilities α of the ions could be determined from the actual densities used.[15] However, the electrostatic potentials at the rubidium (approximately -0.30 a.u.) and chloride-ion sites are close to the values in RbCl, so the standard polarizabilities can be used: 11.33 a.u. for Rb^+ and 19.89 a.u. for Cl^-.[16] The environment of a zinc ion in Rb_2ZnCl_4 should be similar to its environment in $ZnCl_2$. Therefore, 5.33 a.u. was used for the polarizability of Zn^{2+}.[17] Simulations with polarizabilities reduced 25% are presented also, to illustrate the tendencies that existed in the rigid-ion simulation and to explore trends.

The values $a=12$ a.u. and $b=1.2$ for the parameters in Eq. (6) for all three ions were arrived at by trial and prejudice. A value of b close to unity was chosen so that $\mu(\mathcal{E})$ would vary nearly linearly until rollover and saturation. Then a was chosen to make the saturation moment as high as possible without inviting catastrophe, which occurs almost certainly with $a<10$ a.u. for the polarizabilities used. Based on the second hyperpolarizabilities of inert gasses[18] and the way γ varies within an isoelectronic series,[19] we estimate the hyperpolarizabilities should be less than 2000 a.u. for Rb^+, less than 1000 a.u. for Zn^{2+}, and greater than 1000 a.u. for Cl^-. Perhaps γ of Cl^- should be even an order of magnitude larger.[14] For the case of full polarizabilities, the chosen values of a and b give second hyperpolarizabilities 653 a.u., 307 a.u., and 1146 a.u., for Rb^+, Zn^{2+}, and Cl^-, respectively. Figure 1 shows the dipole moments versus field strength for the three ions and indicates the range of the function sampled and average values from the simulation described in Sec. III B. Note that the saturation of the dipole moment is an artifact only, not a required property of the model. It is interesting that the role of a positive second hyperpolarizability in this model is not so much to enhance the ability of the ion to be polarized but to delay attenuation of that ability by the negative fourth hyperpolarizability.

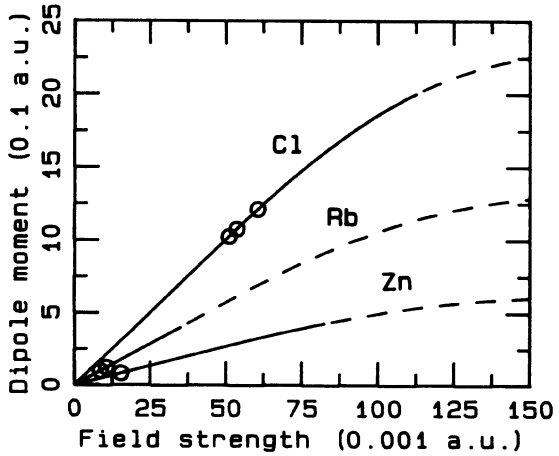

FIG. 1. Dipole moments μ vs field strength $\mathcal{E}$ from Eq. (6). Dashed lines indicate values that were not sampled in the simulation of Sec. III B. Magnitudes of the average moments from that simulation are indicated with circles for the three types of Cl^- site, the two types of Rb^+ site, and the Zn^{2+} site.

Equations (3) and (6) lead to

$$\varepsilon=\frac{\alpha(1+b)}{2a^2}(1-e^{-(a\mathcal{E})^2})-\frac{ab}{2}\mathcal{E}^2e^{-(a\mathcal{E})^2},$$

but, in practice, the first term is rewritten in terms of the hyperbolic sine. The nonlinear Eqs. (2), after substituting Eqs. (4) and (6), are solved at each step of the integration of the equations of motion.

The equations of motion for coordinates are integrated using the Verlet formula.[20] The velocities are updated using Eq. (10c) of Ref. 20 as a corrector in conjunction with the predictor formula (not required in constant lattice simulations)

$$v_+=(x_0-x_-)/t+(5a_0-2a_-)t/6,$$

where the subscripts $-$, 0, and $+$ refer to three successive time steps separated by the interval t; and x, v, and a are a generalized coordinate, its velocity, and acceleration, respectively. Among the highest-frequency modes in Rb_2ZnCl_4 are those involving "breathing" of the tetrahedral ions at about 290 cm^{-1}. In simulations starting from experimental positions with a small amount of kinetic energy, this breathing is the most dominant motion. It can be observed in trajectory "movies" and causes oscillations for a short time in the potential energy versus time. Thus, the estimated breathing-mode frequency with full polarizabilities is about 310 ± 10 cm^{-1}. At these low frequencies, a quite large time step can be used in integrating the equations of motion. We used $t=0.01033$ psec, which is ten of the unit of time that mixed with the atomic mass unit (not atomic unit of mass) gives energy and distance in atomic units.

III. RESULTS AND DISCUSSION

A. Fixed-lattice simulations

The space group *Pnam* is used here to describe the 28-ion, orthorhombic cell of the paraelectric phase of Rb_2ZnCl_4. In that space group, b is the longest axis and c the shortest. The projection of the Zn^{2+} positions in the bc plane has approximate hexagonal symmetry, so the a axis is called the pseudohexagonal axis. The paraelectric phase transforms at $T_I=303$ K to an incommensurate phase then to one and another ferroelectric phase upon cooling.[21] The spontaneous polarization in the higher-temperature ferroelectric phase is parallel to **c**, and the unit cell in that phase is tripled along **a**.

Among the reasons that a simulation with a small sample size can be misleading is that quasistabilizing forces between an ion and its periodic image in another cell are absent because the image is constrained to move with the ion. This problem is magnified when quasirigid molecular ions are involved. Therefore, a supercell of dimensions $2a\times b\times 2c$ (112 ions in $35.002\times24.047\times27.514$ a.u.^{3}) is probably the minimum large enough to make the forces between one $ZnCl_4^{2-}$ ion and its images small compared to forces between it and its neighbors. This supercell was used in fixed-lattice simulations with full and 75% polarizabilities. These simulations were started by adding an amount of kinetic energy that would make the temperature 25 K if that energy was being added to a stable structure. This kinetic energy was added to the average structure of the real solid determined by x-ray scattering.[22]

The paraelectric cell contains two mirror planes at $z=c/4$ and $z=3c/4$. The two mirror planes are equivalent by an inversion through the center of the cell, and each ion can be associated with one mirror plane or the other. One mirror plane from each of the fixed-lattice simulations is shown in Fig. 2. The duration of each of these simulations was 10.33 psec and the temperatures were 380 K using the full polarizabilities and 318 K with the reduced polarizabilities. An ion is represented in these figures by an ellipse centered at the average position with asymmetry in the motion represented by an elongated ellipse.

In the experimentally determined average structure, the two Rb^+ ions and two of the Cl^- ions from each molecule occupy inequivalent sites on a mirror plane, as does the Zn^{2+} ion. The other two Cl^- ions occupy equivalent sites Cl(3) on opposite sides of the mirror plane. Table I compares bond lengths and angles within the simulated $ZnCl_4^{2-}$ ions to experiment. The bonds in the simulations are typically 1% to 2% larger than the experimental values, and reduced polarizabilities appear to increase

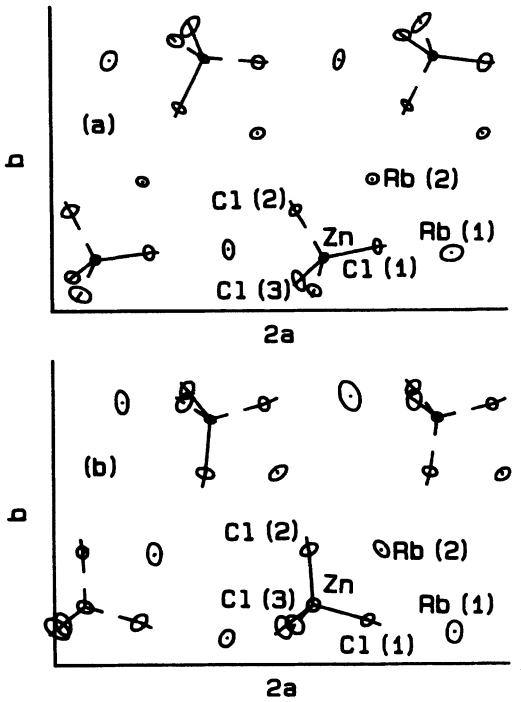

FIG. 2. View parallel to $-$**c** of the mirror plane at $z=c/4$ from a 10.33 psec rigid-lattice simulation with (a) reduced and (b) full polarizabilities. The motion of each ion is represented by an ellipse at the average position. Each average dipole moment is shown as a line (1 a.u. of length to 1 a.u. of moment) from the average position, and the bond vector from each Zn^{2+} to the four nearest Cl^- ions is a solid line if it has a component out of the page or a dashed line if it has a component into the page. There are two equivalent Cl(3) sites in each molecule: one above the mirror plane and one below.

TABLE I. Bond lengths (a.u.) and angles (degrees) (tetrahedral angle is 109.5°) within $ZnCl_4^{2-}$ ion from experimentally determined average positions (Ref. 25), simulation with full polarizabilities (Fig. 4), and simulation with reduced polarizabilities (Fig. 3).

Bond	Experiment	Full	Reduced
Zn—Cl(1)	4.21	4.33	4.31
Zn—Cl(2)	4.26	4.29	4.37
Zn—Cl(3)	4.24	4.31	4.35
Angle	**Experiment**	**Full**	**Reduced**
Cl(1)—Zn—Cl(2)	114.5	110.7	110.6
Cl(1)—Zn—Cl(3)	111.1	109.0	112.9
Cl(2)—Zn—Cl(3)	106.1	110.1	105.7
Cl(3)—Zn—Cl(3)	107.5	107.7	107.5

the bond lengths except in the case of Zn—Cl(1). While the bond lengths in the reduced polarizabilities simulation are farther from the experimental values, they are very close to the sum of the ionic radii for tetrahedral bonding, 4.35 a.u.[23] Too much emphasis should not be placed on this comparison, however, because the experimentally determined structure is an average over time and space of a disordered structure.[24]

The Zn—Cl(1) bonds are almost parallel to **a** according to experiment,[3,22,24] as they appear in Fig. 2(a). However, instead of the Zn—Cl(1) bond being parallel to **a** in the simulation with full polarizabilities, the Zn—Cl(2) bond is nearly aligned with **b**, as can be seen in Fig. 2(b). This characteristic of the simulated solid appears to be more like K_2ZnCl_4 than Rb_2ZnCl_4.[25] This incorrect alignment in the full-polarizabilities simulation appears to be caused by repulsion of an Rb(2) by the moment of a Cl(2). Translation of the Rb(2) causes a rotation of a $ZnCl_4^{2-}$ to which it is bound. The effect of chloride-ion polarizability on the Rb(2) positions can be seen in the views along $-\mathbf{a}$ in Fig. 3(a) and Fig. 4(a). More polarizable anions push Rb(2) farther from being superposed in this view. The positions of Rb(2) in Fig. 3(a) compare more favorably with experiment.

There existed rubidium-induced instabilities in the rigid-ion simulation, which were relaxed by one of two equivalent rotations of the $ZnCl_4^{2-}$ ions about **a**. Those rotations were correlated in two-dimensional networks. The reduced-polarizabilities simulation, Fig. 3(a), has these same instabilities and the correlated rotations that result from them. These instabilities and the associated rotations are present in the simulation with full polarizabilities, Fig. 4(a), but their arrangement into networks is absent. This absence appears to result from frustration by displacements of $ZnCl_4^{2-}$ discussed in the next paragraph.

Figure 3(b), the view along $-\mathbf{b}$ of the reduced-polarizabilities simulation, reveals another structural dependence on the ability of the anions to polarize. The instability of a Cl(1) site caused by electrostatic monopole-monopole interactions with two Zn^{2+} ions in neighboring mirror planes are relaxed by a displacement

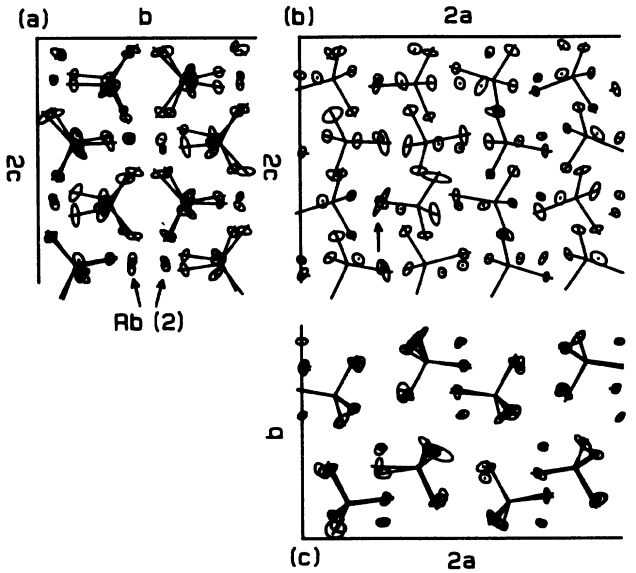

FIG. 3. Views parallel to (a) **a**, (b) $-\mathbf{b}$, and (c) $-\mathbf{c}$ from the 10.33 psec rigid-lattice simulation with reduced polarizabilities. In this and the following figures, the Zn^{2+} ellipses and moments are not shown, and all Zn^{2+}—Cl^- bonds are represented by solid lines. Some Rb(2) sites are indicated in (a) for comparison with Fig. 4(a). An arrow in (b) points to a Cl(1) that hopped through its mirror plane initiating a propagating solitonlike disturbance in the "chain" of correlated Cl(1) ions in line with the arrow.

toward one or the other zinc ions as seen in Fig. 3(b). This displacement, which is correlated with the displacements of equivalent Cl(1) in chains along **c**, causes a large rotation of the $ZnCl_4^{2-}$ ion about **b**. In the rigid-ion simulation of Ref. 1, the Cl(1) kept moving until it reached a zero-field site exactly between the mirror planes.

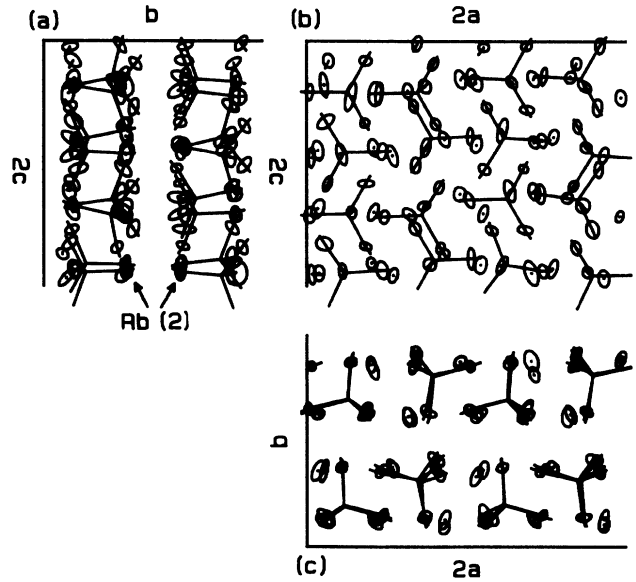

FIG. 4. Views parallel to (a) **a**, (b) $-\mathbf{b}$, and (c) $-\mathbf{c}$ from the 10.33 psec rigid-lattice simulation with full polarizabilities.

A small arrow in Fig. 3(b) points parallel to one of these chains of four Cl(1) (made infinite by the boundary conditions). The Cl(1) at the tip of the arrow jumped through its mirror plane at about 5 psec into the simulation. This created a soliton in that chain of Cl(1) ions that traveled at a velocity of 5.0 bohr/psec through the periodic boundary to the Cl(1) just below the arrow. After passage of the soliton, each of the four Cl(1) ions had jumped from the site below its mirror plane to the equivalent site above.

The zinc-induced instability of Cl(1) is relaxed somewhat differently in the simulation with full polarizabilities, as can be seen in Fig. 4(b). Instead of the rotation about **b** that points the Zn—Cl(1) bond toward one of the destabilizing zinc ions, the whole $ZnCl_4^{2-}$ ion moves out of the mirror plane. A reasonable interpretation of this difference is that a $ZnCl_4^{2-}$ ion with fully polarizable chloride ions avoids pointing its Cl(1) moment toward neighboring zinc ions by not rotating; then it avoids pointing both the Cl(1) and Cl(2) moments at rubidium ions by displacement out of the mirror plane.

The difference between Figs. 3(b) and 4(b) become very significant when considering that the paraelectric phase transforms to a phase that exhibits an incommensurate modulation with wave vector approximately $\mathbf{a}^*/3$. The two rotations in Fig. 3(b), about **a** and **b**, both appear to be all-zone instabilities causing disorder without any tendency toward cell multiplication, so the only mechanism for transformation would be onset of correlation upon cooling. In contrast, the displacements of the $ZnCl_4^{2-}$ ions in Fig. 4(b) appear to be influenced strongly by cell-multiplying instabilities with wave vector parallel to **a**. This suggests another mechanism for the transition: disorder in the form of a temporally and perhaps spatially aperiodic wave that orders eventually as the temperature is lowered. This wave warps the mirror planes to relieve the stress caused by the interactions of Cl(1) and Cl(2) moments with rubidium ions.

B. Simulation with a variable orthorhombic lattice

The forces of constraint necessary to hold the lattice fixed during the fixed-lattice simulations indicated that the c axis should contract. Since such a contraction might stabilize the displacements on the $ZnCl_4^{2-}$ ions out of the mirror planes, a zero-stress simulation is in order. Initial trials indicated positive but soft shear stiffness: Angles between pairs of lattice vectors varied up to 5° from being right angles, but the averages were right angles. Since the dynamics of the lattice vectors themselves are not of great physical significance in a constant-stress simulation and internal stresses cause rotations of the lattice vectors relative to the ionic basis, we performed simulations in which only the lattice-vector lengths were allowed to vary. These constraints allow relaxation of the orthorhombic lattice while preventing rotations and conserving energy and momentum.

Figure 5 shows the view along $-\mathbf{b}$ of averages collected from steps 301 through 500 (two picoseconds beginning after the third) during a simulation with 168 ions ($3a \times b \times 2c$). This simulation was started in the same

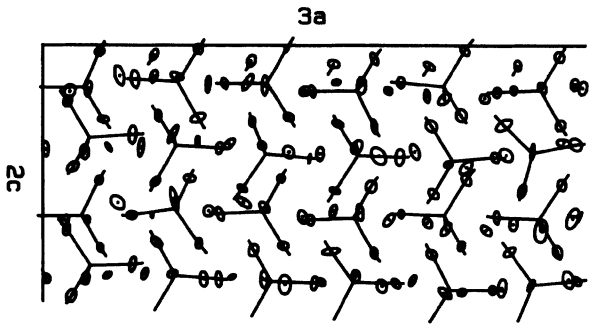

FIG. 5. View parallel to $-\mathbf{b}$ from the final 2.07 psec of a 5.16 psec variable-lattice simulation with full polarizabilities.

way as the fixed-lattice simulations of Sec. III A, and the lattice-vector motion was stopped every 100 steps and the ionic motion restarted with a Maxwell velocity distribution keeping the internal energy constant. This serves to damp lattice oscillations and perhaps provides a better sampling of the ensemble of available states. The temperature during these 5 psec was 453 K, and the respective initial and average lattice constants in a.u. are $a = 17.501$ and 17.593, $b = 24.047$ and 23.514, and $c = 13.757$ and 12.855. The bond lengths and angles during this simulation were essentially the same as in the corresponding fixed-lattice simulation of Sec. III A.

The contraction parallel to **c** has reduced the magnitudes of the $ZnCl_4^{2-}$ displacements out of mirror planes, but modulation of the small displacements in this figure again suggests that they are caused by an instability with a tendency toward cell multiplication parallel to **a**. The half-percent expansion parallel to **a** also suggests that stress within the mirror planes is aiding or is now the primary cause of the displacements. Further evidence of pressure within the mirror planes can be seen in Fig. 1, in which the magnitudes of the average dipole moments from this simulation for each of the three types of Cl^- sites are indicated. The largest average moment in that figure corresponds to the Cl(3) sites, whose moments point generally away from the mirror planes. If the Cl(3) moments are not enhanced by the crystal environment then the Cl(1) and Cl(2) moments are attenuated by it, but the degree of attenuation is minimized by the displacements of the $ZnCl_4^{2-}$ ions from the mirror planes.

The constant b in the simulation is 2.2% too short, which is not surprising since Gordon-Kim forces typically produce an undersized lattice. This has been attributed to excessive exchange energy caused by self-interaction in the local-density approximation that is not balanced by self-interaction in the Hartree energy (however, the assertion that there is no Hartree self-interaction in the Gordon-Kim forces is wrong).[26,6] The c axis in the simulation is 6.6% less than the experimental value. Our inability to reduce this error significantly by adjusting shell charges, polarizabilities, and the other parameters in Eq. (6) leads us to the conclusion that it is also caused by excessive attraction in the tails of the Gordon-Kim potentials. This attraction is likely made more significant in the c direction because of the large separation (7 a.u.) between mirror planes.

IV. SUMMARY

We have used a shell model in conjunction with the electron-gas model of Gordon and Kim to include ionic polarizability in simulations of paraelectric Rb_2ZnCl_4. The natural separation of the pair potentials into electron-electron, electron-nuclear, and nuclear-nuclear parts suggested the representation of an induced dipole moment as a displacement of all the electrons relative to the nucleus. This approximation does not affect the long-range dipole-monopole and dipole-dipole interactions, but does cause extra-stiff short-range and field-gradient interactions. The only requirement over what is needed in a rigid-ion calculation is knowledge of the dipole moments of the ions as functions of applied uniform electric field strength.

A departure of the present calculation from first principles was required because the linear approximation for the $\mu(\mathcal{E})$ and the low symmetry of the solid allowed polarization catastrophe. The cause of polarization catastrophe was found to be induction of huge moments by dipole-dipole interactions so that the moments aligned with the fields of monopoles. Negative curvature in the moment versus field strength at high fields was required to avoid the catastrophe. Therefore, we invented a function that had the proper signs for polarizability and hyperpolarizability and also the required negative curvature at high field strength.

A simulation with the polarizabilities at 75% of their accepted values produced the results expected from the presence of zinc-induced and rubidium-induced instabilities that were discovered in a previously reported rigid-ion simulation. Polarizability of its constituents kept the nonrigid $ZnCl_4^{2-}$ ions intact and they rotated about **a** and **b** to partially relax the instabilities. A soliton occurred in one chain of correlated **b** rotations. The rotations about **b** were removed by turning up the polarizabilities to full strength, but the cost of having the Cl(1) and Cl(2) moments lie in mirror planes, pointing at rubidium ions was so high that the $ZnCl_4^{2-}$ ions moved out of those planes.

The interactions between the chloride-ion moments of one $ZnCl_4^{2-}$ ion and rubidium ions that are bound to other $ZnCl_4^{2-}$ ions give rise to correlated displacements of all ions belonging to one mirror plane. These correlated displacements warp the mirror planes with a cell-multiplying modulation very similar to that which appears in the real crystal as the paraelectric phase is cooled. This modulation should appear as disordered displacements of the $ZnCl_4^{2-}$ ions at high temperatures, with the time between hops very long compared to the duration of these simulations.

ACKNOWLEDGMENTS

Paul Edwardson was supported by the National Research Council and the Naval Research Laboratory during the later part of this work. Work at the University of Nebraska was supported by the U.S. Army Research Office and the Office of Naval Research.

[1]P. J. Edwardson, V. Katkanant, J. R. Hardy, and L. L. Boyer, Phys. Rev. B **35**, 8470 (1987).
[2]J. A. McGinnety, Inorg. Chem. **13**, 1057 (1974).
[3]M. Quilichini and J. Pannatier, Acta Crystallogr. B **39**, 657 (1983).
[4]R. G. Gordon and Y. S. Kim, J. Chem. Phys. **56**, 3122 (1972).
[5]E. Clementi and C. Roetti, At. Data Nucl. Data Tables **14**, 177 (1974).
[6]W. C. Mackrodt and R. F. Stewart, J. Phys. C **12**, 431 (1979).
[7]R. E. Watson, Phys. Rev. **111**, 1108 (1958).
[8]D. A. Liberman, D. T. Cromer, and J. T. Waber, Comput. Phys. Commun. **2**, 107 (1971).
[9]M. Parrinello and A. Rahman, Phys. Rev. Lett. **45**, 1196 (1980).
[10]A. D. Buckingham, Adv. Chem. Phys. **12**, 107 (1967).
[11]G. Jacucci, I. R. McDonald, and A. Rahman, Phys. Rev. A **13**, 1581 (1976).
[12]M. J. L. Sangster and M. Dixon, Adv. Phys. **25**, 247 (1976).
[13]M. P. Tosi and M. Doyama, Phys. Rev. **160**, 716 (1967).
[14]P. W. Langhoff, J. D. Lyons, and R. P. Hurst, Phys. Rev. **148**, 18 (1966).
[15]H. Bilz, G. Benedek, and A. Bussmann-Holder, Phys. Rev. B **35**, 4840 (1987).
[16]S. S. Jaswal and T. P. Sharma, J. Phys. Chem. Solids **34**, 509 (1973).
[17]J. Tessman, A. Kahn, and W. Shockley, Phys. Rev. **92**, 890 (1953).
[18]D. P. Shelton, J. Chem. Phys. **84**, 404 (1986); I. Cernusak, G. H. F. Diercksen, and A. J. Sadlej, Phys. Rev. A **33**, 814 (1986).
[19]G. Maroulis and D. M. Bishop, J. Phys. B **18**, 3653 (1985).
[20]D. Beeman, J. Comp. Phys. **20**, 130 (1976).
[21]P. Muralt, E. Voit, and R. Kind, Phys. Status Solidi B **119**, K65 (1983), and references therein.
[22]V. Day, private communication.
[23]C. Kittel, *Introduction to Solid State Physics,* 5th ed. (Wiley, New York, 1976), p. 100.
[24]K. Itoh, A. Hinasada, H. Matsunaga, and E. Nakamura, J. Phys. Soc. Jpn. **52**, 664 (1983).
[25]F. Milia, R. Kind, and J. Slak, Phys. Rev. B **27**, 6662 (1983).
[26]A. I. M. Rae, Chem. Phys. Lett. **18**, 574 (1973).